ON THE TRANSITION FROM LOCAL REGULAR TO GLOBAL IRREGULAR FLUCTUATIONS[1]

Patrick Pintus[2] Duncan Sands[3] Robin de Vilder[4]

N° 9617

First version: January 1996
This version: September 1996

[1]Robin de Vilder dedicates this paper to the loving memory of his wife Annemiek. The authors gratefully acknowledge the intellectual support and guidance of Jean-Michel Grandmont and Sebastian Van strien. Also many thanks to Ale-Jan Homburg, Floris Takens and Marcello Viana for interesting discussions and helpful suggestions.

[2]EHESS and CEPREMAP (Paris, France). E-mail: pintus@cepremap.msh-paris.fr.

[3]Unversité d'Orsay (Orsay, France). E-mail: sands@topo.math.u-psud.fr.

[4]University of Amsterdam (the Netherlands). E-mail: robin@fwi.uva.nl.

On the Transition from Local Regular to Global Irregular Fluctuations

ABSTRACT. We present a general framework for understanding the transition from local regular to global irregular (chaotic) behaviour of nonlinear dynamical economic models in discrete time. The fundamental mechanism is the unfolding of quadratic tangencies between the stable and the unstable manifolds of periodic saddle points. We apply these methods to the infinite horizon model of Woodford [33], amended by Grandmont, Pintus and de Vilder [16] to account for capital-labour substitution.

JEL classification numbers: C61, E32.

Keywords: nonlinear dynamics, homoclinic bifurcations.

La Transition de Trajectoires Locales Régulières vers des Trajectoires Globales Irrégulières

RÉSUMÉ. Nous proposons un cadre général permettant d'appréhender le phénomène de transition vers des trajectoires irrégulières ("chaotiques"), dans les systèmes dynamiques non-linéaires en temps discret. Le mécanisme fondamental à l'œuvre dans ce processus est l'apparition de points de tangence quadratique entre les variétés stable et instable de points-selle périodiques. Nous appliquons ces méthodes au modèle à horizon infini de Woodford [33] dans lequel la substitution capital-travail a été introduite, suivant Grandmont, Pintus et de Vilder [16].

Classification du JEL: C61, E32.

Mots-clé: dynamique non-linéaire, bifurcations homocliniques.

1 Introduction

We present a general framework for understanding the transition from local regular to global irregular (chaotic) behaviour of nonlinear dynamical economic models in discrete time. The fundamental mechanism is the unfolding of quadratic tangencies between the stable and the unstable manifolds of periodic saddle points, created for example through the Hopf bifurcation or the flip (period doubling) bifurcation. Numerical evidence that an invariant circle created in a Hopf bifurcation may transform into a strange attractor has already been reported by Brock and Hommes [7], Dana and Malgrange [10], Goeree, Hommes and Weddepohl [13] and Medio and Negroni [22].

By applying recent results from the theory of higher-dimensional nonlinear dynamical systems to a two-dimensional model, de Vilder [30, 31] showed that homoclinic bifurcations of the stable and unstable manifolds of the *autarkic steady state* guarantee complicated global fluctuations[1]. The present article is a extension of de Vilder [30] and shows that these phenomena occur more generally when homoclinic bifurcations indeed involve *periodic* saddles.

We shall illustrate these results by studying the dynamics arising in the infinite horizon model of Woodford [33], amended by Grandmont, Pintus and de Vilder [16] to account for capital-labour substitution. The latter authors have shown that two local bifurcations occur in this model: a Hopf bifurcation and a flip bifurcation, both creating periodic saddles. We shall show that for parameters "far away" from the bifurcation point, the global dynamics may become very irregular.

2 The Model and Local Results

2.1 The Economy

We follow the lines set out in Woodford [33] and Grandmont, Pintus and de Vilder [16]. The economy consists of two classes of infinitely long living agents, called workers and capitalists, both acting in perfectly competitive markets and having perfect foresight. Preferences of both groups of agents are represented by separable utility functions. Each period, a perishable consumption good is produced from labour and capital. Moreover, there is a constant supply of outside money $M > 0$.

[1]That homoclinic bifurcations of stable and unstable manifolds of a steady state also arise in different types of economic models has recently been reported by Brock and Hommes [7].

Workers may be identified by a representative agent who works, consumes and maximizes

$$\sum_{t=1}^{+\infty}[\beta_w^{t-1}U(c_t^w) - \beta_w^t V(l_t)] \tag{1}$$

where $0 < \beta_w < 1$, c_t^w and l_t denote respectively the workers' discount factor, the amount of consumed good and the amount of labor supplied in period t. In this paper we will use as utility functions

$$U(c) = \frac{(c/B)^{1-\alpha_2}}{1-\alpha_2},\ V(l) = \frac{l^{1+\alpha_1}}{1+\alpha_1}, \tag{2}$$

where $B > 0$ is a scaling parameter and $\alpha_1 > 0$, $\alpha_2 > 0$ represent the constant elasticities of marginal utility of leisure and consumption.
Let M_{t-1}^w and k_{t-1}^w be respectively nominal money and capital stock held by the representative worker at the outset of period t. At time t the agent faces on $c_t^w \geq 0, k_t^w \geq 0, M_t^w \geq 0$ and $l_t \geq 0$ the following constraints:

$$p_t c_t^w + p_t k_t^w + M_t^w = M_{t-1}^w + (r_t + (1-\delta)p_t)k_{t-1}^w + w_t l_t, \tag{3}$$

$$p_t c_t^w + p_t k_t^w \leq M_{t-1}^w + (r_t + (1-\delta)p_t)k_{t-1}^w \tag{4}$$

where $p_t > 0$ is the price of the produced good, $w_t > 0$ is the nominal wage paid, $r_t > 0$ is the nominal return on capital and δ is the fixed depreciation rate of capital equipment. The constraint (3) is the usual budget constraint while (4) is an additional financial constraint which has the following interpretation: the worker has to finance his consumption and capital purchases by either money held in that period or by returns on capital. He cannot however finance them by wage income. This imperfection in the financial market is the result of asymmetric information: both labor and capital revenues are received at the end of the period, but only the latter can warrant a productive capital secured loan. That is, the fact that future labor income depends on hidden actions or hidden information prevents the worker from borrowing against his human capital.

We assume that the following inequalities hold in equilibrium:

$$U'(c_t^w) > \beta_w R_{t+1} U'(c_{t+1}^w), \tag{5}$$

$$\omega_t U'(c_t^w) > \beta_w V'(l_t), \tag{6}$$

where $R_{t+1} > 0$ stands for $r_{t+1}/p_{t+1} + 1 - \delta$, i.e. the real gross return on capital, while ω_t stands for the real wage, i.e. w_t/p_t. Condition (5) states that the workers choose not to hold productive capital, hence $k_t^w = 0$ for all t, whereas condition (6) ensures that the financial constraint (4), which becomes a Clower constraint because of (5), is binding for all dates.

The labor choice of the worker is therefore the solution of the problem

$$\max\ \{U(c_{t+1}^w) - V(l_t)\} \text{ such that } p_{t+1}c_{t+1}^w = w_t l_t. \tag{7}$$

As in an overlapping generations model with two periods, the workers' labor supply is described, when interior, by the first order condition:

$$v(l_t) = u(\frac{w_t l_t}{p_{t+1}}), \tag{8}$$

where $u(c) \equiv cU'(c)$, $v(l) \equiv lV'(l)$, $\gamma \equiv u^{-1} \circ v$ being the function whose graph is the offer curve. A straightforward computation gives the constant elasticity of γ with respect to l, i.e. $\varepsilon_\gamma = (1 + \alpha_1)/(1 - \alpha_2)$. Using eq. (8), the elasticity of labor supply ε_l with respect to the real wage is obtained, i.e. $\varepsilon_l = (1-\alpha_2)/(\alpha_1+\alpha_2)$. We shall focus on the case where the optimal labor supply is an increasing function of the real wage, i.e. $\varepsilon_\gamma > 1$. An equivalent way of saying this is that the two goods in the model, i.e. leisureand consumption, are gross substitutes.

Capitalists may also be represented by a single agent who maximizes

$$\sum_{t=1}^{+\infty} \beta_c^{t-1} \ln c_t^c, \tag{9}$$

where $0 < \beta_c < 1$ is the capitalists' discount factor, c_t^c is the agent's consumption of the good. By assuming that workers discount future utilities more than capitalists (i.e. $0 < \beta_w < \beta_c < 1$) it follows that at the steady state and thus locally near by, inequalities (5) and (6) hold. In addition, we assume that capitalists never hold money but only productive capital[2], i.e. they will choose $c_t^c \geq 0$ and $k_t^c \geq 0$ so as to maximize their discounted utility subject to

$$p_t c_t^c + p_t k_t^c = (r_t + (1 - \delta)p_t)k_{t-1}^c. \tag{10}$$

It follows that

$$c_t^c = (1 - \beta_c)R_t k_{t-1}, \; k_t = \beta_c R_t k_{t-1}. \tag{11}$$

Since capital is only held by capitalists, we may drop the superscript for k.

Finally, as in Grandmont, Pintus and de Vilder [16], we assume that the two input goods in the production process, labor and capital, are used in variable proportions: positive elasticity of substitution is allowed in the technology $F(k_{t-1}, l_t)$. In fact, we use the CES production function

$$F(k, l) = A[sk^{-\eta} + (1 - s)l^{-\eta}]^{-1/\eta}, \tag{12}$$

where $A > 0$ is a scaling parameter, $0 < s < 1$ governs the capital share in total income and $\eta > -1$, whereas the elasticity of input substitution is $\sigma = 1/(1 + \eta)$.

[2]We can again invoke an imperfection in information: while owning the whole capital stock and organizing production, capitalists are however unable to finance investment other than out of their own revenues from productive capital, i.e. loan contracts from workers to capitalists are unenforceable. Workers are then unable to invest even indirectly in productive capital by lending to capitalists.

Let us fix some notation: we denote the capital-labor ratio by a, i.e. $a_t \equiv k_{t-1}/l_t$. Since we allow for substitution between capital and labor and have constant returns to scale, we write competitive real gross returns on capital and the real wage as functions of a, i.e. $R_t \equiv R(a_t)$ and $\omega_t \equiv \omega(a_t)$. Defining $f(a) \equiv F(k,l)/l$ as output per unit of labor, we have

$$\rho(a) \equiv R(a) - (1-\delta) = F_k(k,l) = f'(a),\ \omega(a) = F_l(k,l) = f(a) - a\rho(a). \tag{13}$$

The elasticity of input substitution σ is given by the elasticity of a with respect to the ratio ω/ρ.

Next we define, as in Benhabib and Laroque [6], the intertemporal equilibria[3] of our economy:

Definition 2.1 *An intertemporal competitive equilibrium with perfect foresight is a sequence* $(c_t^w, c_t^c, l_t, k_{t-1}, \omega_t, \rho_t, p_t)$ *in* $\mathbf{R}_{++}^7$, $t = \ldots, -1, 0, 1, \ldots$, *such that:*

1. (c_{t+1}^w, l_t, M) *is an optimal choice of workers at date* t, *given* (ω_t, p_t, p_{t+1}),
2. (k_t, c_t^c) *is an optimal choice of capitalists at date* t, *given* R_t,
3. (k_{t-1}, l_t) *maximizes the profit of the entrepreneur at date* t, *given* (ρ_t, ω_t),
4. *Markets clear at all dates.*

Although from definition 2.1 it might appear that one needs seven variables to fully describe the model at time t, it turns out that the dimension of the problem can be reduced to two, as shown by the following definition.

Definition 2.2 *An intertemporal competitive equilibrium with perfect foresight is a sequence* (a_t, k_{t-1}) *in* $\mathbf{R}_{++}^2$, $t = \ldots, -1, 0, 1, \ldots$ *such that*

$$\begin{cases} \omega(a_{t+1})/a_{t+1} &= \gamma(k_{t-1}/a_t)/(\beta_c R(a_t) k_{t-1}), \\ k_t &= \beta_c R(a_t) k_{t-1}. \end{cases} \tag{14}$$

Remarks: The previous definition states that eq. (14) summarizes the intertemporal equilibria (equilibria for short) of the model. Note that the dynamical system has only dimension two, instead of three in an overlapping generations structure with outside money and capital-labor substitution, as in Benhabib and Laroque[4] [6].
Moreover, the first order conditions for workers and capitalists, i.e. the Euler equations, are only

[3] We only consider non-autarkic intertemporal equilibria.

[4] The interpretation of money is not the same in both models, see Grandmont, Pintus and de Vilder [16].

necessary and a study of the global dynamics of an infinite horizon model has to pay attention to all the conditions for an optimal sequence. On the one hand, because of the binding liquidity constraint, the infinitely long living worker behaves just like a young worker in an overlapping generations structure, so no transversality condition is required to describe the optimal choice of the worker. On the other hand, along an optimal path for capitalist's choice, $k^{opt} = (\ldots, k_0^{opt}, k_1^{opt}, \ldots)$, the transversality condition reads

$$\lim_{t\to+\infty} \beta_c^t \left(\frac{R_t}{R_t k_{t-1}^{opt} - k_t^{opt}}\right) k_{t-1}^{opt} = 0. \tag{15}$$

From the second part of eqs. (11) we have a candidate for the optimal positive k_t^{opt}, which satisfies the Euler equation, as easily checked. Substituting this candidate into eq. (15), we then know that the transversality condition is satisfied. By using Mangasarian's Lemma it follows that the sequence k given in eq. (11) is optimal.

We are now in a position to study the behavior of the dynamical system in eq. (14). The first step is to find its stationary point(s). It follows from definition 2.2 that the steady states (a^s, k^s) in $\mathbf{R}^2_{++}$ must satisfy

$$\omega(a^s) = \frac{\gamma(k^s/a^s)}{k^s/a^s}, \quad \text{with } R(a^s) = \frac{1}{\beta_c} \text{ or } \rho(a^s) = \frac{1}{\beta_c} + \delta - 1. \tag{16}$$

We fix the parameters $A = (\delta + 1/\beta_c - 1)/s$, $B = (\delta + 1/\beta_c - 1)(1-s)/s$ and α_1 close enough to zero, and vary the parameters η (or σ) and α_2 (or ε_γ). For this choice of parameters a straightforward computation shows that, independent of the values of η and α_2, there exists a unique interior (monetary) steady state $(a^s, k^s) = (1, 1)$.

2.2 Local dynamics

In Grandmont, Pintus and de Vilder [16] it is shown that endogenous fluctuations are a possible outcome of the dynamical system in eq. (14). In order to be self contained we briefly recall those results from their paper that are needed in understanding some of the phenomena arising in the global dynamics of the model. We fix a value for the elasticity of input substitution σ (or equivalently for η) and investigate how the dynamical system depends on ε_γ (or α_2 since α_1 is fixed). From eqs. (2), (8), (12), (13), one easily derives the following expression for eqs. (14) as functions of the parameters.

$$\begin{cases} a_{t+1}^{-1}(s a_{t+1}^{-\eta} + 1 - s)^{-1-1/\eta} = (k_{t-1}/a_t)^\gamma k_t^{-1}, \\ k_t = \beta(sA a_t^{-\eta-1}(s a_t^{-\eta} + 1 - s)^{-1-1/\eta} + 1 - \delta) k_{t-1}. \end{cases} \tag{17}$$

We denote by G_{ε_γ} the map defining the dynamical system near the steady state, with parameter ε_γ, of the form $(a_{t+1}, k_t) = G_{\varepsilon_\gamma}(a_t, k_{t-1})$ and derived from eqs. (17), when $\varepsilon_\omega(a^s) \neq 1$ at the steady state, i.e. $\eta \neq (1-s)/s$. Grandmont, Pintus and de Vilder [16] show that the family G_{ε_γ} undergoes two types of local bifurcations as ε_γ increases from 1 to $+\infty$:

Proposition 2.1 *Assume $\theta(1-s)/s < 1$, where $\theta = 1-\beta_c(1-\delta)$. Then the following holds:*

1. *If $\sigma \in [0.\theta(1-s)/2]$ then a stable supercritical Hopf bifurcation occurs at $\varepsilon_{\gamma H} = (s-\sigma)/(\theta(1-s)-\sigma)$; for ε_γ slightly larger than $\varepsilon_{\gamma H}$ an attracting invariant closed curve surrounds the unstable steady state on which the dynamics is either periodic or quasi-periodic, see figure 1a.*

2. *If $\sigma \in (\theta(1-s)/2, \sigma_H)$ then a stable supercritical Hopf bifurcation occurs at $\varepsilon_{\gamma H}$, followed by an unstable subcritical flip bifurcation at $\varepsilon_{\gamma F} = (2s+\theta(1-s)-2\sigma)/(2\sigma-\theta(1-s)) > \varepsilon_{\gamma H}$, where $\sigma_H = s[1+\theta(1-s)/s-\sqrt{1-\theta(1-s)/s}]/2$; for ε_γ slightly larger than $\varepsilon_{\gamma H}$ an attracting invariant closed curve surrounds the unstable steady state on which the dynamics is either periodic or quasi-periodic, see figure 1a, while for ε_γ slightly smaller than $\varepsilon_{\gamma F}$ close to the unstable steady state there exists a period two saddle, see figure 1b.*

3. *If $\sigma = \sigma_H$, there exists a value ε_γ such that both a stable Hopf bifurcation and a unstable period-doubling bifurcation occur; this is a so-called degenerate local bifurcation[5], see figure 1c. The Hopf and flip bifurcations occur at $\varepsilon_\gamma = \varepsilon_{\gamma H}$ and $\varepsilon_\gamma = \varepsilon_{\gamma F}$.*

4. *If $\sigma \in (\sigma_H, \sigma_F)$ then an unstable subcritical flip bifurcation occurs at $\varepsilon_\gamma = \varepsilon_{\gamma F}$, where $\sigma_F = [\theta + s(1-\theta)]/2$; for ε_γ slightly smaller than $\epsilon_{\gamma F}$ close to the stable steady state there exists a period two saddle, see figure 1b.*

In order to investigate the global dynamical behavior of the aggregate economy, we set the values of the various parameters as follows:

$$s = 1/3,\ \delta = 1/10,\ \beta_c = 1.$$

Notice that for this value of β_c we are actually considering the limit case where capitalists do not consume. We emphasize that the results of this paper can also be obtained for β_c values different from 1[6]. For these values of s and δ, the upper bounds for σ in order to get local bifurcations is $\sigma_H \approx 0.05$ for the Hopf bifurcation and $\sigma_F = 0.2$ for the flip bifurcation[7]. Hence, deterministic and stochastic endogenous fluctuations in a competitive economy occur for low values of the elasticity of input substitution.[8]

[5]Both eigenvalues go through -1 at the same time. This case is one of the (nongeneric) strong resonance configurations.

[6]Indeed, β_c must be close enough to one to guarantee that gross investment, although positive at the steady state, remains positive along orbits far away from the steady state such as those considered in the next section.

[7]These values of σ correspond in magnitude to the ones reported by Reichlin [27] and Benhabib and Laroque [6].

[8]Recent findings of Cazzavillan, Lloyd-Braga and Pintus [8] and Cazzavillan and Pintus [9] show that internal or external increasing returns to scale are an essential feature to obtain endogenous fluctuations with relatively high input substitution.

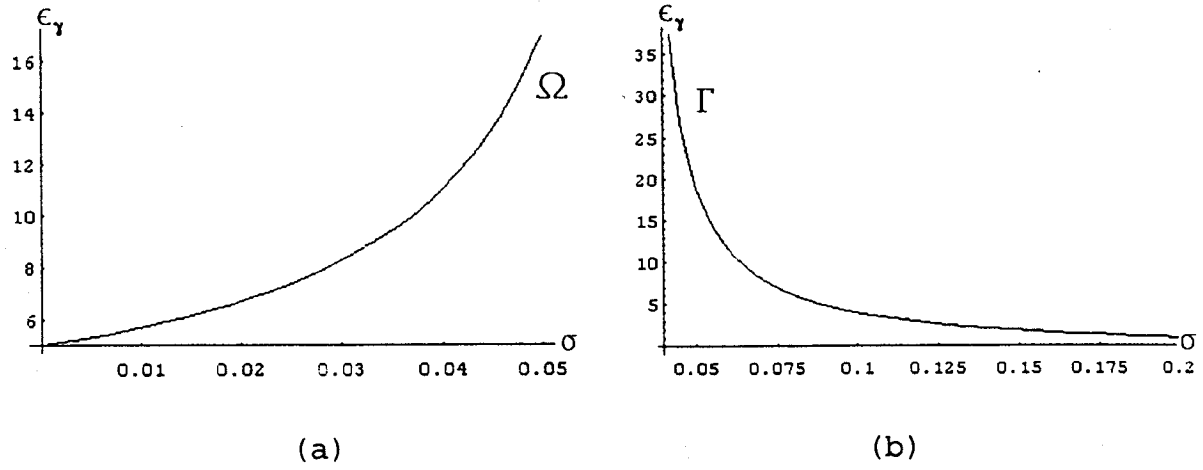

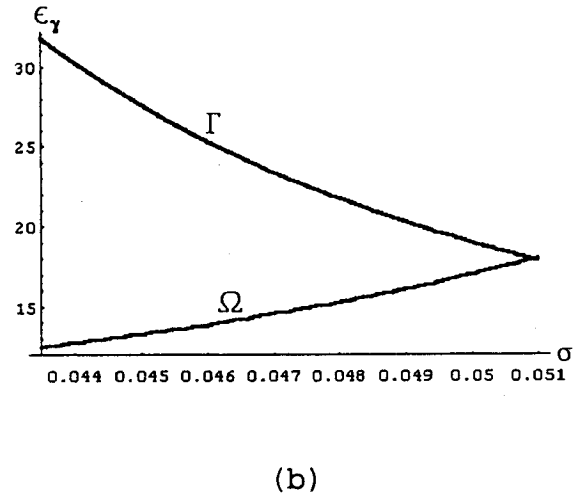

Figure 1: (a) The curve Ω in parameter space along which the stable Hopf bifurcation occurs: for parameter values below but close to Ω the fixed point is attracting whereas an attracting invariant circle surrounding the repelling monetary steady state exists for parameter values just above Ω. (b) The curve Γ in parameter space along which the period-doubling bifurcation occurs: for parameters just above Γ the fixed point is a saddle whereas for parameters slightly below Γ a period 2 orbit surrounds the attracting monetary steady state. (c) The curves Ω and Γ. For $\sigma \approx 0.051$ the period-doubling and Hopf bifurcations coincide; this gives rise to a co-dimension two local bifurcation.

3 Global Analysis

In this section we will give a global analysis of the perfect foresight dynamics given by eq. (17). Since many economists may not be familiar with the methods of global analysis used in this section, we introduce each concept before making use of it. In each case our goal has been to provide a framework within which the presented results can be understood.

We analyse the behaviour of a variety of dynamical objects including invariant circles and stable and unstable manifolds. Our techniques can be applied to any two-dimensional dynamical system satisfying the appropriate mathematical conditions. The conditions specific to each section are listed there and can all be checked either by hand or with the help of a computer.[9] If these conditions are not satisfied then the results may not be valid. The following conditions are common to all sections.

> The dynamical system G must be a C^3 diffeomorphism in a neighbourhood of the object (invariant circle etc.) studied. This means that there should be an open set U containing the object such that the restriction of G to U is one-to-one, has its first three derivatives continuous and has non-zero Jacobian determinant everywhere in U. Moreover, G must have C^3 dependence on any parameters varied.

These conditions are satisfied by the dynamical system studied in this paper. Eq. (14) depends C^3 on its parameters and defines a C^3 diffeomorphism on the following set:

$$0 < a^{**} \equiv [s/((1-s)(\theta(1+\eta)-1))]^{1/\eta} < a < a^{*} \equiv [\eta s/(1-s)]^{1/\eta}, \tag{18}$$

$$\begin{aligned} 0 &< k < [\beta_c a^{\gamma} R(a)\omega(a^{*})/(Ba^{*})]^{1/(\gamma-1)}, \\ 0 &< k < [(\beta_c a^{**} R(a^{**}))^{\gamma}\omega(a)/(Ba)]^{1/(\gamma-1)}. \end{aligned} \tag{19}$$

These curves were obtained by calculating those (k, a) values for which the Jacobian determinant of eq. (14) is zero or has a singularity, i.e. becomes infinite. We then checked that eq. (14) is invertible on the set given by eqs. (18) and (19) (this does not follow automatically from the fact that the Jacobian determinant is non-zero there).

All the phenomena and analysis described in this chapter occur inside this set. Outside this set (where G is not invertible) the dynamical structure seems to be even more complicated. Unfortunately, the mathematics needed to analyse this behaviour does not yet exist.

[9] Using the program DUNRO [11] for example.

3.1 Arnol'd Tongues

We start with some numerical observations. Fix $\sigma = 0.025$ and increase γ starting from 7.0. With this choice of σ the Hopf bifurcation occurs at $\gamma = 7.4$. If, with $\gamma < 7.4$, we orbit a point then it is attracted to the monetary steady state (figure 1a). If $\gamma > 7.4$ is close to 7.4, then points we orbit are attracted, in general, to a small invariant circle (figures 1a and 5a). If we alter γ then the motion on the circle seems to change. However for some exceptional γ values larger than and close to 7.4 we see no invariant circle. Any points we iterate are attracted to a periodic orbit (figure 4a). If we alter γ by a small amount then we continue to see an attracting periodic orbit. Such attracting periodic orbits occur more frequently as γ increases. As γ increases the invariant circle grows.

These phenomena are due to the presence of "Arnol'd tongues" in the parameter space of our system (see Guckenheimer and Holmes [17, Section 6.2]). Arnol'd tongues occur in any generic two or more parameter system in which there is a Hopf bifurcation. It is easier to understand what is happening if two parameters are varied rather than just one. We shall therefore vary σ and ε_γ. Recall that Hopf bifurcations occur along the curve Ω in the $(\sigma, \varepsilon_\gamma)$ plane described in the last section (proposition 2.1). Along this curve, the eigenvalues at the monetary steady state are complex and of magnitude one. Their argument is a real number in 0 to 2π, varying with the position on the curve. Consider a point ω on Ω. There are two cases depending on whether the argument ρ at ω is a rational or irrational multiple of 2π: if it is irrational then a curve known as an Arnol'd hair emanates from ω in the $(\sigma, \varepsilon_\gamma)$-plane, on the side of Ω on which the invariant circles exist, see figure 2a. For each parameter on this hair the invariant circle has the same rotation number; this rotation number is equal to ρ. In fact the hair consists of exactly those parameters near ω for which the rotation number is equal to ρ. Because ρ is irrational the motion on the invariant circles is quasi-periodic: there are no periodic points.

The other case occurs when ρ is a rational multiple of 2π: in this case a so-called Arnol'd tongue emanates from ω as in figure 2b. Near Ω, neither tongues nor hairs overlap though they do occur arbitrarily close to each other. The Arnol'd tongue consists of exactly those parameters near ω for which the rotation number is equal to ρ. Unlike an Arnol'd hair, a tongue has non-empty interior. The boundary of the tongue near ω consists of smooth curves which come together in a cusp like way at ω, see figure 2b. Since ρ is rational, say $\rho = s/r$, each invariant circle corresponding to a parameter in the tongue contains orbits of period r. All points on the invariant circle converge to one of these orbits of period r.

For a parameter in the interior of the tongue and close to ω the invariant circle contains exactly two periodic orbits, both of which are hyperbolic. In the invariant circle, one of these orbits is attracting and the other repelling (cf. figure 3b). In our system, the periodic orbit which is repelling in the invariant circle is actually a saddle: one of its eigenvalues has magnitude greater than 1

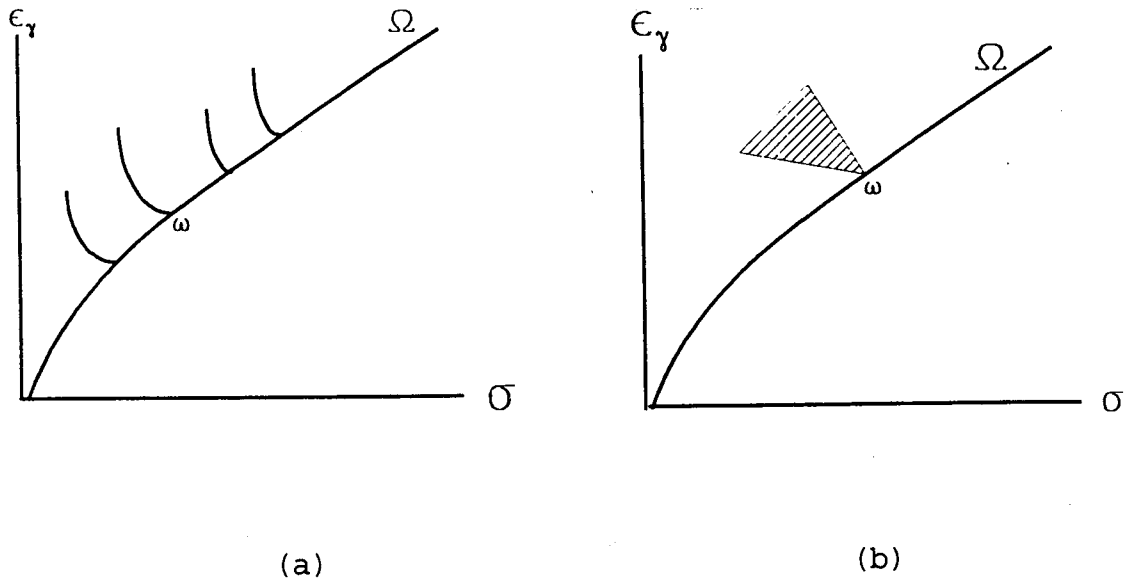

Figure 2: (a) Schematic drawing of Arnol'd hairs. A hair consists of those parameters near ω for which the rotation number on the circle is equal to ρ, where ρ is irrational. (b) Schematic drawing of an Arnol'd tongue. The tongue consists of those parameters near ω for which the rotation number on the circle is equal to ρ, where ρ is rational.

(corresponding to the eigenvector tangent to the invariant circle) and the other has magnitude less than one (corresponding to the eigenvector which is transversal to the invariant circle, because the circle is attracting). The periodic orbit which is attracting in the invariant circle is actually a sink: it attracts nearby points both on and off the invariant circle.

As the parameter is changed so as to cross the boundary of the tongue near but not at ω, the periodic orbits approach each other, becoming less and less hyperbolic until, on the boundary of the tongue, they merge to form a single non-hyperbolic periodic orbit of period r in a (reverse) saddle-node bifurcation (cf. figure 3a-c): on the boundary of the tongue, near but not at ω, the invariant circle contains only one periodic orbit, which is non-hyperbolic and of period r. Beyond the boundary of the tongue, outside but close to the tongue, there are no longer any orbits of period r in the invariant circles.

These results enable us to explain the numerical obervations described at the start of this section. For $\varepsilon_\gamma < 7.4$ we are on the side of Ω for which there is just an attracting fixed point (figure 1a). For $\varepsilon_\gamma > 7.4$ we are on the side of Ω for which there are Arnol'd tongues and Arnol'd hairs; the fixed point has become repelling and there is an invariant circle around it. If $(\sigma, \varepsilon_\gamma)$ lies in a tongue then the circle is "invisible": we only see a periodic attractor. This is the periodic sink inside the invariant circle described above. If we iterate a typical point then it converges to this sink and we see neither the invariant circle nor the other periodic orbit lying within it (the periodic saddle). For example, $(\sigma, \varepsilon_\gamma) = (0.025, 7.42)$ lies inside the tongue corresponding to rotation number $1/5$. Figure 4a shows

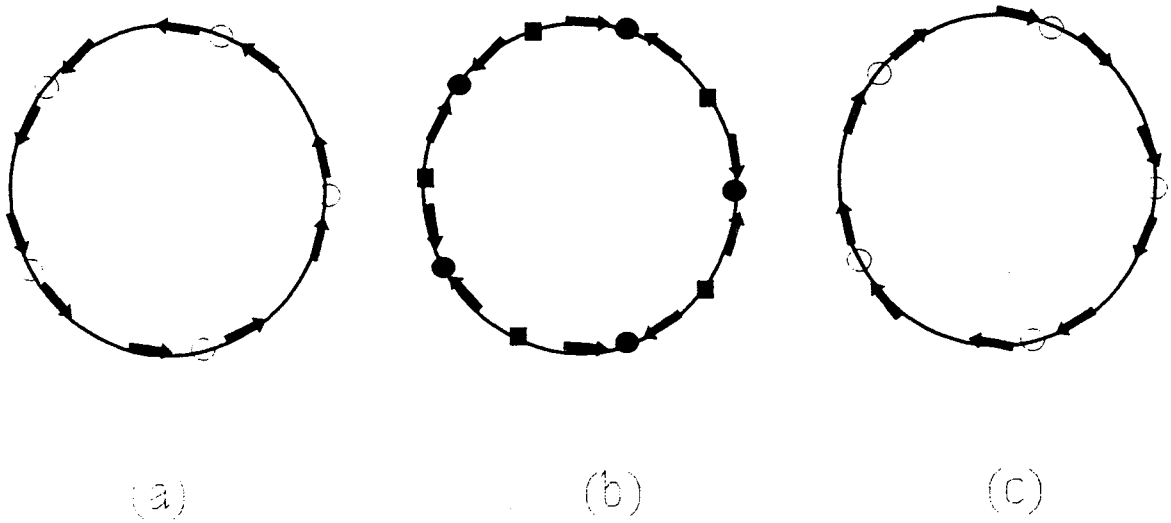

Figure 3: If the parameter is varied near Ω so as to completely traverse an Arnol'd tongue with rotation number $\rho = 1/5$ the overall scenario is as follows: (a) at the first boundary of the tongue the invariant circle contains a unique and non-hyperbolic periodic orbit, of period 5. (b) The periodic orbit splits apart as the parameter moves into the interior of the tongue through a saddle-node bifurcation, giving two hyperbolic orbits of period 5, one attracting in the circle, the other repelling in the circle. (c) as the parameter approaches the other boundary of the tongue this pair of periodic orbits is destroyed in a reversed saddle-node bifurcation; at the other boundary the invariant circle contains a unique and non-hyperbolic periodic orbit, of period 5.

the result of iterating a point: it is attracted to the period 5 sink. The theoretical results described above tell us that this sink together with a periodic saddle lies in an invariant circle. In figure 4b we show the period 5 saddle-sink pair and in figure 4c the invariant circle, both calculated using the program DUNRO [10] [11]. If we change ε_γ by a small amount then we continue to see a period 5 sink since we will not have moved out of the tongue, see figure 4d. This is a general phenomenon: when there is a periodic orbit, it persists for nearby parameter values: tongues have width. The thinner a tongue is, the quicker it is crossed as ε_γ is varied. Tongues are thin close to Ω; they are also thin if the corresponding periodic orbits have high period, the most extreme example of which is given by Arnol'd hairs which can be thought of as corresponding to periodic orbits of infinite period and have no width at all.

If $(\sigma, \varepsilon_\gamma)$ lies on a hair then we see an invariant circle. The dynamics on the circle is quasi-periodic and the rotation number changes the moment ε_γ is changed. In spite of hairs being thin and tongues thick, quasi-periodic motion is seen quite often since the set of all hairs can be shown to have positive Lebesgue measure, so the probability of $(\sigma, \varepsilon_\gamma)$ lying on a hair is positive. Close to Ω this probability approaches 1. This explains why, as ε_γ is increased past 7.44, we see mainly quasi-periodic motion on the (small) invariant circle and, occasionally and for a short period of time, high-period sinks as we cross one of the many thin tongues near Ω, see figures 5a-b. The fact that the circle grows as ε_γ is increased past 7.4, at least for ε_γ close to 7.4, is a general property of supercritical Hopf bifurcations.

3.2 Homoclinic Bifurcations and Circle Breakup

The above description only applies when the parameters are near the bifurcation curve Ω: there the invariant set created in the Hopf bifurcation is homeomorphic to a circle, and the dynamics on it is conjugate to either an irrational rotation on the circle (quasi-periodic motion) or every point is attracted to a periodic orbit. It is also possible to follow tongues far away from Ω. In this case a great variety of exotic phenomena may occur, the invariant circle may break up and tongues may overlap[11].

Let us first present some numerical results for our model (eq. (17)) to show the sorts of phenomena that can occur when the parameters are moved far away from Ω. We shall focus on the cases where $\sigma = 0.025$ and $\sigma = 0.05$ and investigate how the dynamics depends on ε_γ. From proposition 2.1 we know that for these choices of σ the Hopf bifurcation occurs for $\varepsilon_\gamma = 7.4$ and $\varepsilon_\gamma = 17$, respectively.

[10] In fact, all the computations concerning the global analysis were performed with the program DUNRO [11].

[11] One may wonder if the dynamical system in eq. (14) continues to represent the actual dynamic behavior of the model, presented in section 2, *along orbits far away from the steady state*. Indeed, we have degrees of freedom to ensure that, along the orbits considered in the sequel, the inequalities (5) and (6) are satisfied, i.e. that the savings structure does not change along those orbits: given γ, α_1 must be sufficiently close to 0 and α_2 close enough to 1, while β_w must be small enough.

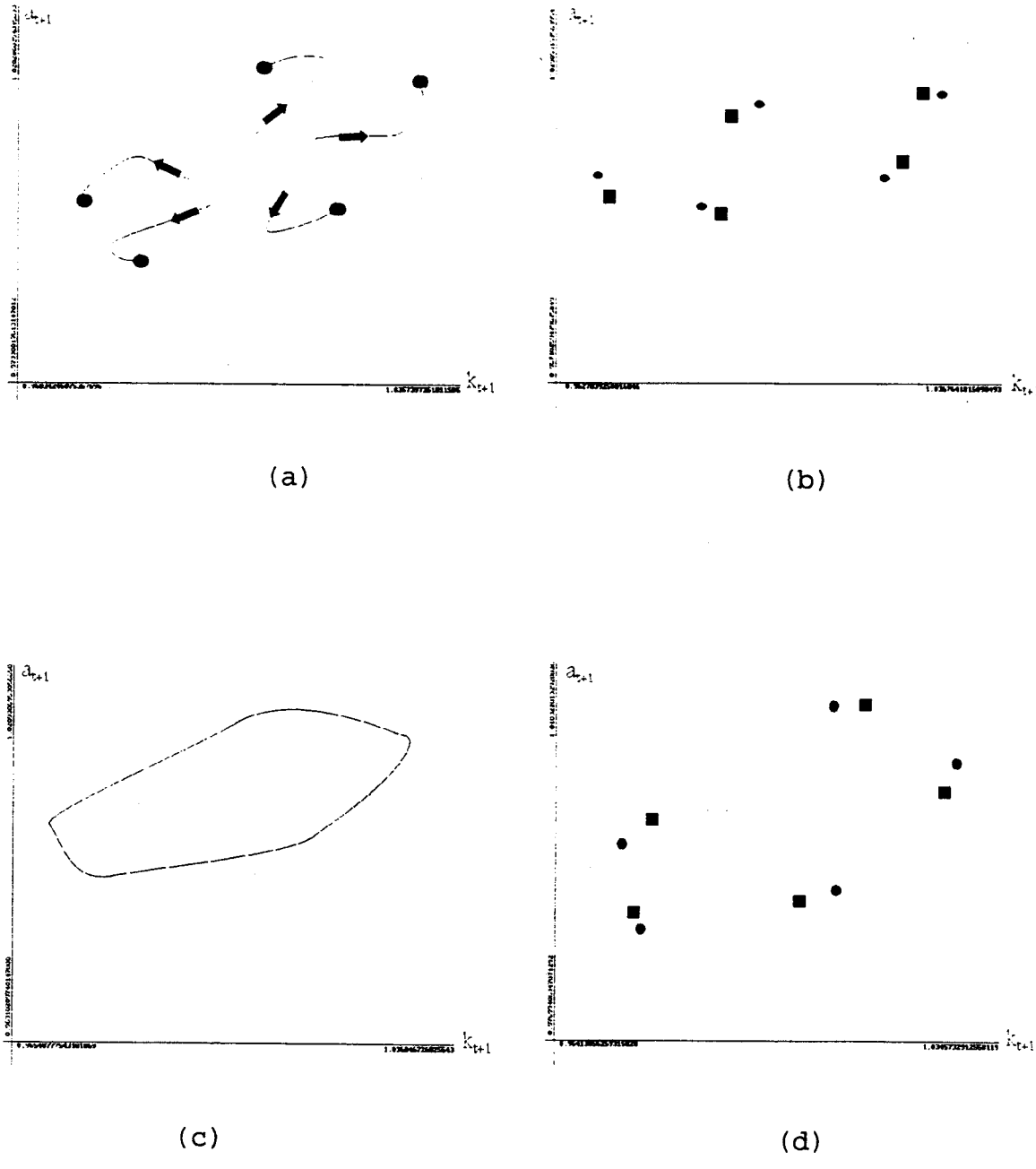

Figure 4: (a) Iterating a point close to the monetary steady state results in an orbit that converges to the period 5 sink; (b) This period 5 sink (marked with dots) is accompanied by a period 5 saddle (marked with squares); (c) Although in numerical experiments one only observes the period 5 sink the period 5 saddle-sink actually lies inside an invariant circle; (d) By increasing the parameter ε_γ the period 5 saddle-sink pair persists, though the relative position of the dots and squares has changed compared to (b) (cf. figure 3(a-c)).

In addition, from proposition 2.1 it follows that for $\sigma = 0.05$ an unstable period-doubling bifurcation arises for $\varepsilon_\gamma = 19$.

Case 1 ($\sigma = 0.025$): To follow the evolution of the equilibrium dynamics of the model for increasing values of ε_γ we present the phase portraits for different values of ε_γ in figure 5. The corresponding output time series may be found in figure 6. As may be expected from the above discussion the dynamics of the model displays (quasi) periodic behaviour for ε_γ values close to the bifurcation value (see figures 5a-b and 6a-b): we are crossing different tongues and hairs so the rotation number changes between rational and irrational. Observe from figure 5b that the invariant set looks like a deformed circle; this does not prevent the dynamics from being homeomorphic to a rational or irrational rotation of the circle. This picture changes completely if the parameter ε_γ is increased further: the smooth invariant set transforms into a seemingly strange attractor, see figure 5c-d. If we look at the corresponding output time series in figure 6c-d we observe a mixture of regular and irregular behaviour. This pattern in the output time series may be understood as follows. Take, for example, the invariant set presented in figure 5d. In this case the invariant set consists of 9 pieces; each piece is mapped into itself after 9 steps. It is straightforward to check that in these 9 steps a piece goes around the center of the broken-up circle twice: the rotation number on the invariant set is $\rho = 2/9$. It is this property that accounts for the regularity in the time series of figure 6d. To explain the irregularity of the output series we zoom into one of the nine pieces of the attractor presented in figure 5d, see figure 7a; each piece displays the same complicated geometric structure. The time series on the attractor of figure 7a displays very irregular and seemingly unpredictable behaviour, see figure 7b. This accounts for the irregularity of the output time series in figure 6d. The pattern seen in the time series (6c) for the attractor of figure 5c can be explained similarly.

Case 2 ($\sigma = 0.05$): We next consider the case when $\sigma = 0.05$. We again follow the evolution of the equilibrium dynamics in phase space for increasing values of ε_γ. As in case 1 the dynamics on the invariant set created in the supercritical Hopf bifurcation is homeomorphic to a rational or irrational rotation on the circle for parameters sufficiently close to the bifurcation value, see figure 8a. Notice from figure 8a that the invariant circle is highly stretched in the vertical direction; it is nonetheless very likely that the rotation on the circle is (quasi) periodic. If we look at the time series on the attractor of figure 8a we observe a mixture of periodic and quasi-periodic behaviour (cf. figure 8c). If we further increase ε_γ the invariant set grows and finally disappears, see figure 8b. If we look at the output time series for the attractor presented in figure 8b we observe that it displays a mixture of periodic, quasi-periodic and irregular behaviour, see figure 8d. A closer inspection of the breaking up process of the invariant set reveals that a similar mechanism as in case 1 is at work; for reasons of brevity we omit a detailed description.

For both cases the invariant sets created in the Hopf bifurcations are smooth for parameters close to the bifurcation value, slowly transform with increasing parameters and finally end up as strange

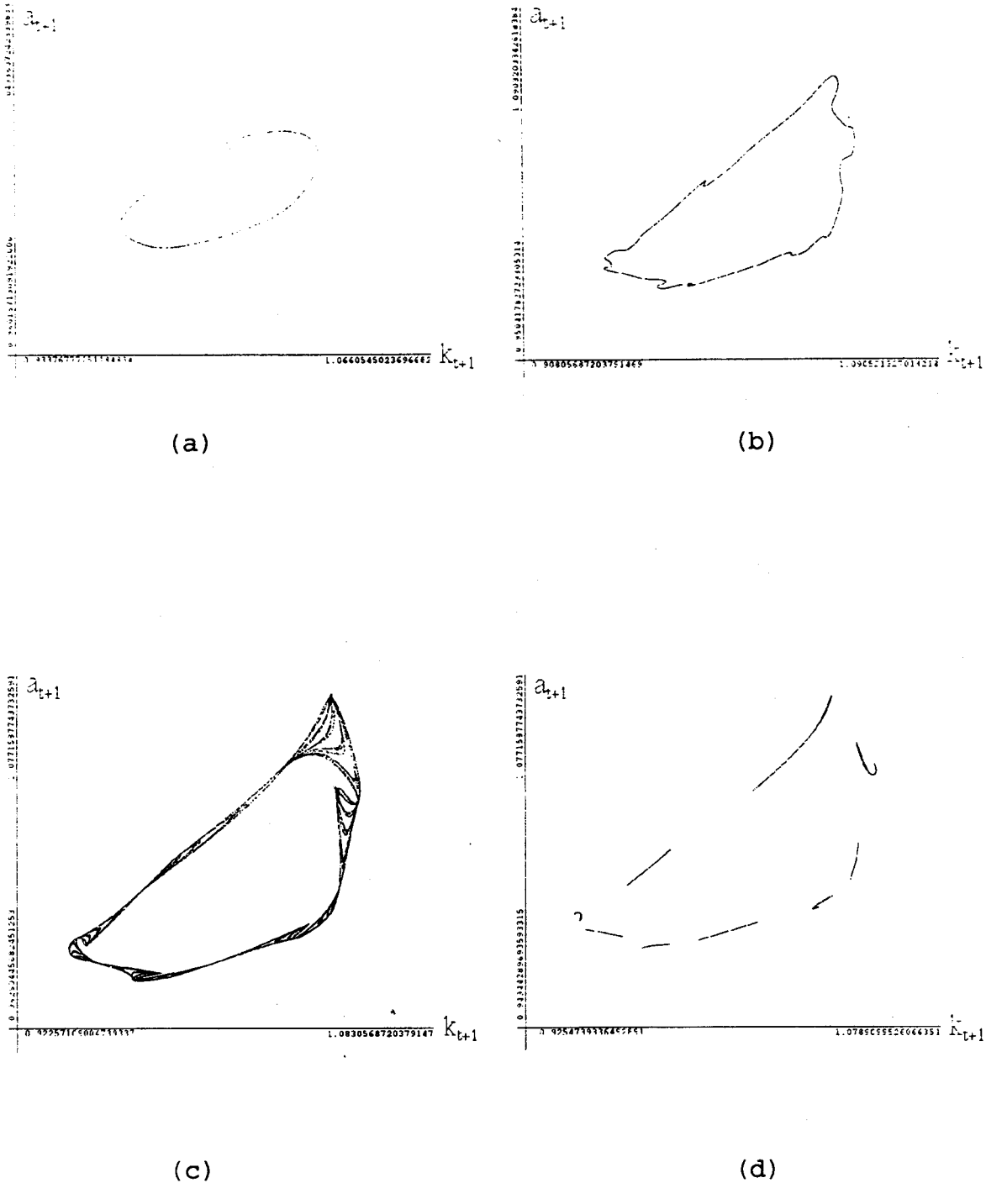

Figure 5: With $\sigma = 0.025$ and increasing values of ε_γ the invariant set created in the Hopf bifurcation is first a smooth circle (a-b) and then transforms into a strange attractor (c-d). We have obtained these figures by iterating an initial state, close to the monetary steady state, approximately 500,000 times.

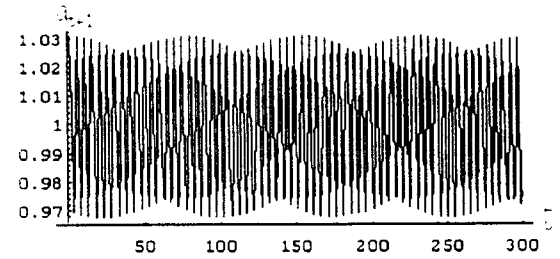

(a)

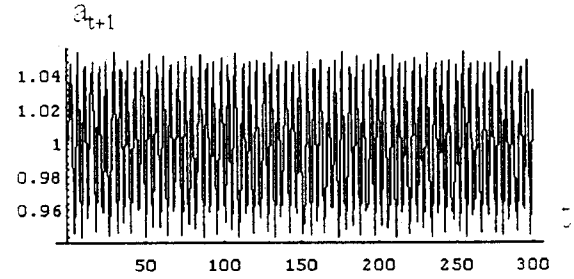

(b)

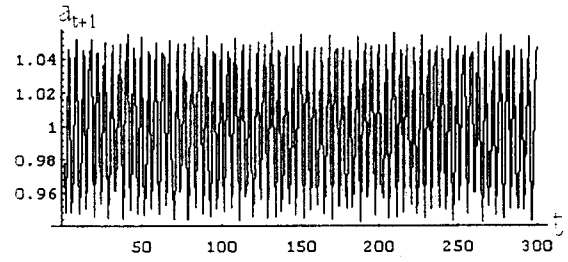

(c)

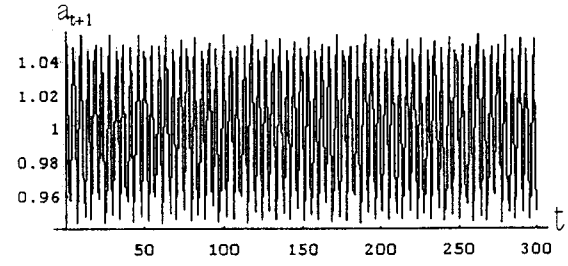

(d)

Figure 6: The output time series for the attractors of figure 5.

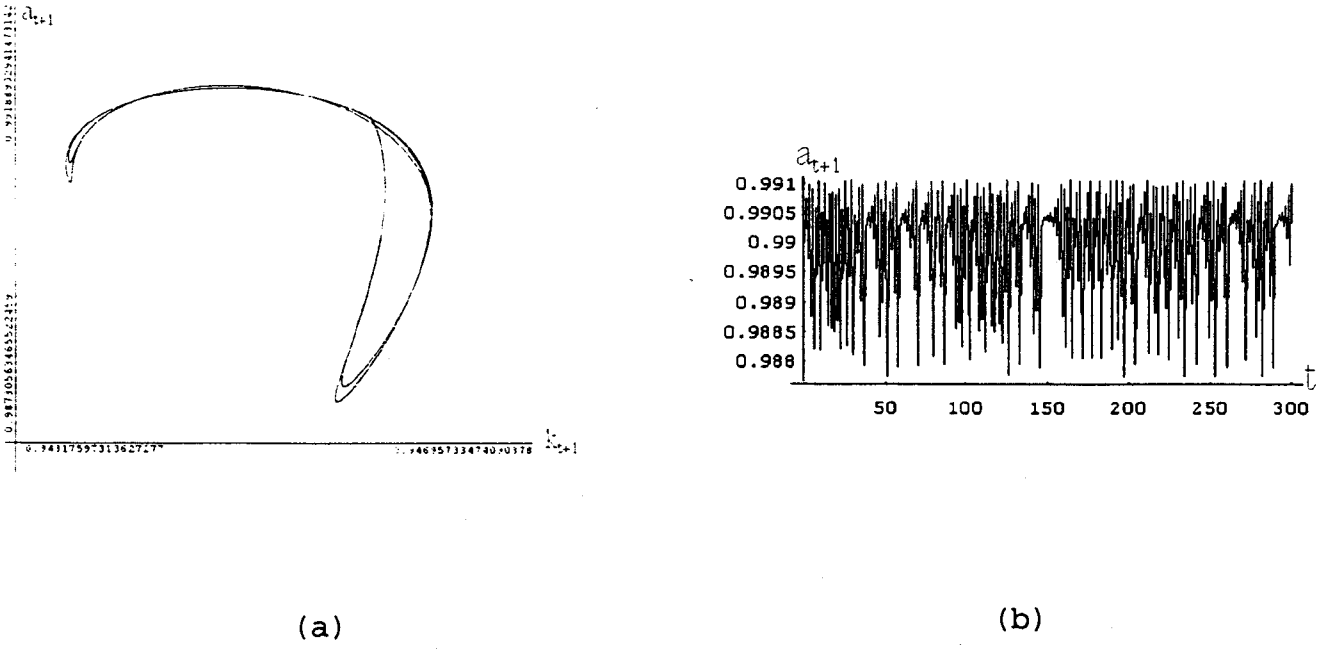

Figure 7: (a) enlargement of one piece (the most left one) of the nine piece strange attractor of figure 5d and (b) the corresponding output time series.

attractors; the corresponding time series first display regular behaviour and end up displaying irregular behaviour. This is known as circle breakup.

The first detailed description of this process was given by Aronson, Chory, Hall and McGehee [2]. In their very interesting paper these authors were able to show that Arnol'd tongues also persist for parameters far away from the Hopf bifurcation curve, but for these parameters Arnol'd tongues tend to overlap, giving rise to non-unique rotation numbers on the invariant set. In addition, inside a tongue and sufficiently far away from the bifurcation curve, they numerically observe period-doubling bifurcation cascades and the appearance of strange Hénon-like attractors. A further understanding of these numerical observations has been given by de Vilder [31, ch. 4 section 4.3]. By applying recent results from the theory of higher-dimensional dynamical systems this author was able to relate the numerical results to the unfolding of so-called homoclinic bifurcations. This is the subject of the rest of this section.

To explain the mechanism that leads to the destruction of the invariant circles and the corresponding creation of strange attractors we need to introduce the notion of stable and unstable manifolds. Suppose p is a hyperbolic fixed point of a diffeomorphism G of the plane, so $G(p) = p$ and the Jacobian $DG(p)$ has no eigenvalues of magnitude 1. The stable manifold of p is the set

$$W^s(p) = \{x \ ; \ G^n(x) \to p \text{ as } n \to \infty\}.$$

If p is a sink then $W^s(p)$ is an open set containing p. If p is a source then $W^s(p)$ only contains p. If p is a saddle then $W^s(p)$ is a smooth one-dimensional curve passing through p (this is why $W^s(p)$ is called the stable *manifold* of p: it is a smooth curve).

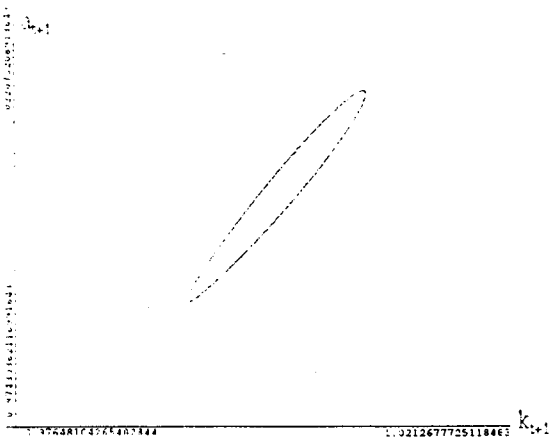

(a)

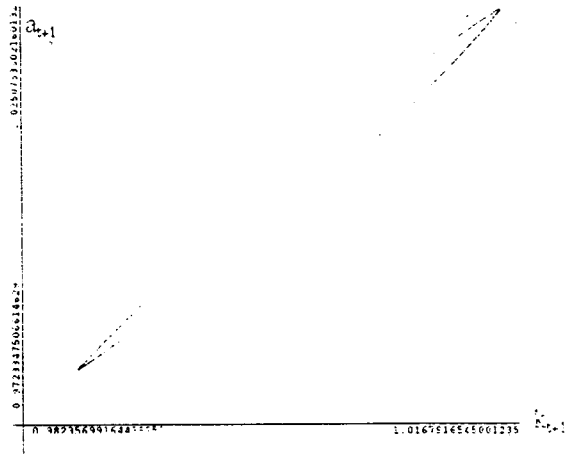

(b)

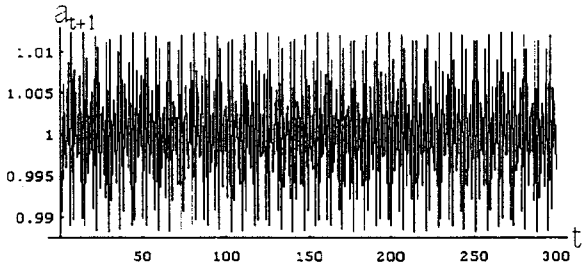

(c)

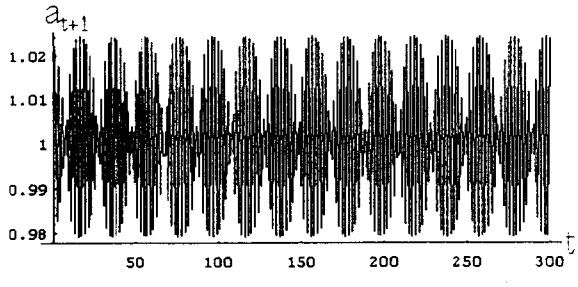

(d)

Figure 8: With $\sigma = 0.05$ and increasing values of ε_γ the invariant set created in the Hopf bifurcation, which is highly stretched in the vertical direction is first smooth (a) and then transforms into a strange attractor (b). The time series on the attractors are presented in c-d.

The unstable manifold is the set

$$W^u(p) = \{x \ ; \ G^n(x) \to p \text{ as } n \to -\infty\}.$$

Here are some examples. If $G(x,y) = (2x, y/3)$ then $W^s(0,0) = \{(0,y) \ ; \ y \in \mathbf{R}\}$, the y-axis. In general if G is linear then $W^s(0,0)$ is the span of the (generalized) eigenspaces corresponding to eigenvalues of magnitude less than 1, known as the stable eigenspace of the linear map. If $(0,0)$ is a saddle then this is a straight line passing through $(0,0)$. Similarly $W^u(0,0)$ is the span of the generalized eigenspaces corresponding to eigenvalues of magnitude greater than 1, the unstable eigenspace of the linear map G: if $G(x,y) = (2x, y/3)$ then $W^u(0,0) = \{(x,0) \ ; \ x \in \mathbf{R}\}$, the x-axis. The stable and unstable manifolds let one see which points go where under the action of G, even for points far away from p. With $G(x,y) = (2x, y/3)$, points just to the left of $W^s(0,0)$ first approach $(0,0)$ closely before being swept off along $W^u(0,0)$ towards $x = -\infty$, $y = 0$. Points just to the right of $W^s(0,0)$ end up going towards $x = +\infty$, $y = 0$.

The importance of stable and unstable manifolds comes from the fact that they are global and not local: they do not just depend on the behaviour of G near p. This is particularly clear when G is non-linear, as it is for our system in eq. (17). Whether G is linear or not, near p its dynamics is conjugate to the dynamics of $DG(p)$ near $(0,0)$. Moreover, $W^s(p)$ is always tangent at p to the stable eigenspace of $DG(p)$ though in general not equal to it (and $W^u(p)$ is tangent to the unstable eigenspace of $DG(p)$). Outside a neighbourhood of p however, this linear-like behaviour no longer occurs: $W^u(p)$ and $W^s(p)$ may even intersect, as in figure 9d. This complicated configuration is remarkably common (cf. Guckenheimer and Holmes [17, p. 22], or de Vilder [30]).

The situation is similar if p is a periodic point rather than fixed. If p has period r then its stable and unstable manifolds are formally defined as:

$$W^s(p) = \{x \ ; \ G^{rn}(x) \to p \text{ as } n \to +\infty\}$$

and

$$W^u(p) = \{x \ ; \ G^{rn}(x) \to p \text{ as } n \to -\infty\}.$$

Each of these is a smooth curve in the plane passing through p, tangent to the stable and unstable eigenspaces of $DG^r(p)$ respectively. Writing $P = \{p, G(p), \ldots, G^{r-1}(p)\}$ for the periodic orbit generated by p, we define the stable manifold of P to be

$$W^s(P) = \bigcup_{k=0}^{r-1} W^s(G^k(p))$$

and the unstable manifold as

$$W^u(P) = \bigcup_{k=0}^{r-1} W^u(G^k(p)).$$

Finding stable and unstable manifolds in analytic form is usually not possible, though they can be calculated numerically up to any prescribed accuracy, see Homburg [18] and Homburg, Sands and de Vilder [19].

Non-trivial points of intersection of stable and unstable manifolds are known as homoclinic points. These are those points x for which $G^n(x) \to p$ as $n \to +\infty$ and as $n \to -\infty$. Formally, if $P = \{p, G(p), \ldots, G^{r-1}(p)\}$ is a periodic saddle orbit and the stable and unstable manifolds of $G^i(p)$ intersect at a point $x \neq G^i(p)$ then x is called a *homoclinic point* of $G^i(p)$. If this intersection is transversal (i.e. $W^s(p)$ and $W^u(p)$ are not tangent at x) then x is called a *transversal homoclinic point*; if the intersection is tangential then x is called a point of *homoclinic tangency.*

The orbit of a homoclinic point is called a *homoclinic orbit*; each point in it is homoclinic. If the stable and unstable manifolds of a periodic saddle point p have points of homoclinic intersection then it follows that the stable and unstable manifolds of each of the other points in the periodic orbit of p also have homoclinic points (cf. Aronson, Chory, Hall and McGehee [2]).

We remarked above that when there is a homoclinic point then the configuration of stable and unstable manifolds is very complicated. Maps with homoclinic points have correspondingly complicated dynamics. In fact, it has been shown by Smale [28] that whenever the stable and unstable manifolds of a (periodic) saddle point p have a point of transversal homoclinic intersection then close to this point of intersection there exists an invariant Cantor set Λ of Lebesgue measure zero (known as a Smale horseshoe)[12] consisting of countably infinitely many periodic orbits as well as uncountably infinitely many aperiodic orbits, of which uncountably infinitely many have dense orbits. Typically, points in Λ have extremely irregular, chaotic orbits. Since Λ is not attracting and in fact has a saddle structure, its long term influence on the dynamics is limited: a point near but not in Λ will in general start by orbiting chaotically, but will rapidly leave the region in which Λ controls the dynamics, and may for example end up being attracted to a periodic sink: the effect of Λ is transient (cf. Guckenheimer and Holmes [17, Section 5.1], Wiggins [32, Section 4.1]).

A completely different picture is obtained in the creation of new transverse homoclinic points via a homoclinic tangency, in going from having no point of homoclinic intersection to having a point of transversal intersection for example. The typical situation is illustrated in figure 9: as a parameter, say γ, is increased, transverse homoclinic points are created. This is a homoclinic bifurcation and has many consequences, perhaps the least of which is that there are Smale horseshoes for every parameter immediately following the one for which the homoclinic tangency occurs.

[12] A Cantor set is an uncountable, compact, totally disconnected set without any isolated points. For example, the set obtained by removing the middle third of the segment $[0, 1]$ and then the middle thirds of the two remaining segments, and so on, is a Cantor set. It has Lebesgue measure zero.

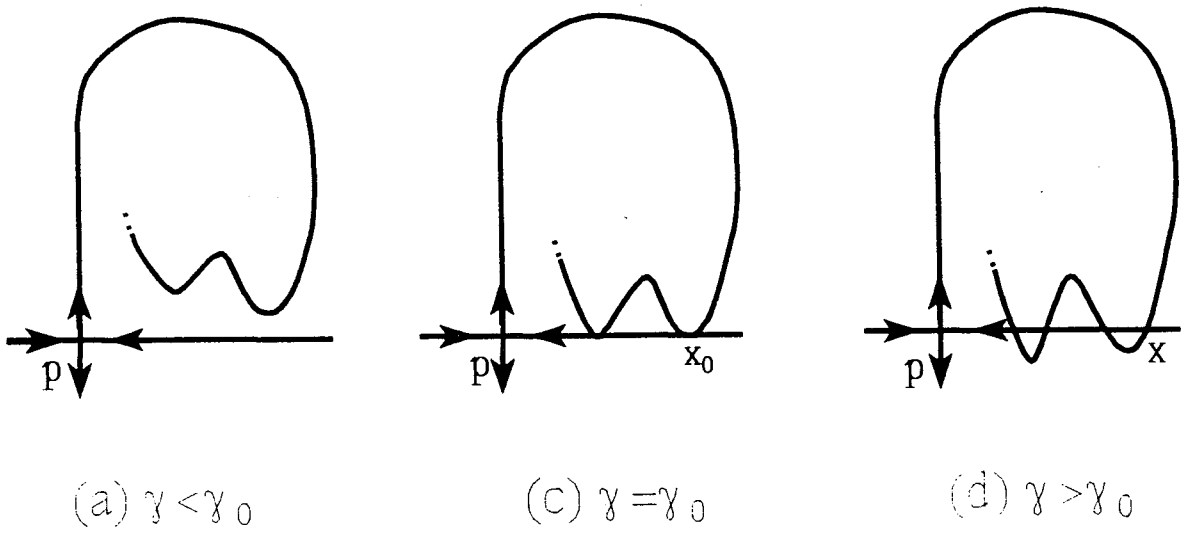

Figure 9: In (a) the stable and unstable manifolds of a fixed saddle point have no points of non-trivial intersection, whereas in (b) there is a point x_0 of tangential contact; finally in (c) there are points of transversal intersection.

In the following we will suppose that

- the product of the eigenvalues evaluated at the periodic saddle p lies inside the unit circle, i.e. $|\det DG^r(p)| < 1$.
- the stable and unstable manifolds move through each other at the tangency in a non-degenerate manner as the parameter is varied.
- the tangential contact is quadratic.

Concerning the above assumptions we remark that the first one is automatically satisfied whenever the saddle is in the (attracting) invariant circle created in the Hopf bifurcation, whereas the second and third assumption are generic. If the above assumptions are met it can be shown that in the creation of transverse homoclinic points through a homoclinic tangency at least three types of important dynamical phenomena arise, each occurring close to the homoclinic tangency:

1. *The Newhouse phenomenon:* There are uncountably many parameters for which G has an infinite number of periodic sinks (see Newhouse [24], Palis and Takens [25, Theorem 1 p. 129 and Appendix 4], Palis and Viana [26, Main Theorem p.207, remarks p.208 and 249]). The point is that for these parameters the map has an infinite number of attracting periodic orbits at the same time. This is quite different to the Smale horseshoe where there are an infinite number of *saddle* periodic orbits. Since the Newhouse sinks attract points, they have a long-term influence on the dynamics. A consequence is that given any (large) N, an interval of parameters can be found such that for every parameter in the interval the map has at least N periodic sinks at the

same time. That is, one should expect to see many periodic sinks. Intuitively, one can think of the Newhouse phenomenon as occuring at those parameters at which an infinite number of Arnol'd tongues overlap.

2. *Hénon-like strange attractors:* There is a set E of parameters with positive Lebesgue measure such that G_{ε_γ} has a strange attractor A_{ε_γ} for each $\varepsilon_\gamma \in E$ (see Mora and Viana [23, Theorem A p. 2 and Section 2], based on Benedicks and Carleson [4], Palis and Takens [25, pp. 140-1]).[13] A typical such Hénon-like strange attractor is illustrated in figure 7a. Each A_{ε_γ} attracts an open set of points and thus influences the dynamics. It can be shown that there are no attracting periodic orbits in A_{ε_γ} and that the dynamics of A_{ε_γ} is chaotic. It has recently been announced by Baladi and Viana [3] that such attractors are stochastically stable and therefore robust: they persist when the system is subjected to a small amount of noise.

3. *Period-doubling and period-halving bifurcation cascades:* There are an infinite number of period-doubling and period-halving bifurcation cascades. By a period-doubling bifurcation cascade we mean the following phenomenon: there is a periodic point which, as the parameter increases, undergoes a period-doubling bifurcation; as the parameter increases further, the period-doubled orbits undergo an additional period-doubling; and subsequent period-doublings occur infinitely often as the parameter increases to some limit parameter. A period-halving bifurcation cascade corresponds to the same phenomenon but when the parameter is decreased; this looks like successive period-halvings if the parameter is increased (see Yorke and Alligood [34], Kan, Koçak and Yorke [21], Palis and Takens [25, p. 40]).

In summary, associated with the generic unfolding of tangential homoclinic intersections, one expects the occurrence of the Newhouse phenomenon, strange Hénon-like attractors and cascades of period-doubling and halving bifurcations. For a more detailed description of the above phenomena we suggest the reader refer to Guckenheimer and Holmes [17], Palis and Takens [25], de Vilder [31] or Wiggins [32].

If the product of the eigenvalues evaluated at the periodic saddle p lies outside the unit circle, i.e. $|\det DG^r(p)| > 1$, then these results hold for the inverse G^{-1} of G, so G will have an infinite number of periodic Newhouse repellors (when G^{-1} satisfies the Newhouse phenomenon), Hénon-like strange repellors, and so forth.

Let us continue with some numerical examples illustrating these ideas, before formalizing them.

Case 1 (continued) ($\sigma = 0.025$): Recall that the invariant set of figure 5d consists of 9 pieces: each piece is mapped in 9 steps into itself. Therefore, one expects the presence of a period 9 saddle. Using

[13] By a strange attractor, we mean a compact invariant set which attracts an open set of points and contains a dense orbit with a positive Lyapunov exponent.

the program DUNRO [11] we were able to find such a period 9 saddle orbit. Again using the program DUNRO [11], which implements the method of Homburg, Sands and de Vilder[14] [19] we calculated the stable and unstable manifolds of this periodic saddle orbit for two values of ε_γ, see figure 10. Observe from figures 10a and 10c that outside the 9 saddle points itself the stable and unstable manifolds of the period 9 saddle do not intersect whereas in figures 10b and 10d they do intersect outside the 9 saddle points: there are transverse homoclinic points and therefore Smale horseshoes.

Case 2 (continued) ($\sigma = 0.05$): The most prevalent feature of the attractor presented in figure 8a-b is clearly its stretched form. It turns out that this particular shape of the attractor is due to the presence of a periodic orbit of period 2 that surrounds the invariant circle. As may be recalled from proposition 2.1, this period two orbit is created in a subcritical period-doubling bifurcation: for parameters larger than $\varepsilon_{\gamma F} = 19$ the steady state is a saddle whereas for parameters slightly smaller than $\varepsilon_{\gamma F}$ the steady state is a repellor surrounded by the orbit of period 2. The period 2 orbit has a saddle structure and continues to exist for parameters as small as $\varepsilon_\gamma = 17$ (where the steady state loses stability through a Hopf bifurcation). There therefore exists an interval of ε_γ values in $[17, 19]$ for which the invariant sets created in the Hopf bifurcation and period-doubling bifurcation co-exist. In figure 11a we present the situation in phase space shortly after the Hopf bifurcation has occurred: the unstable manifolds of the period 2 saddle wrap around the attracting invariant circle whereas the stable manifolds wander off. If we further increase the value of ε_γ we observe from figure 11b that the stable and unstable manifolds of the period 2 saddle orbit have changed position; the stable manifolds now converge to the monetary steady state and the unstable manifolds wander of. Clearly, the stable and unstable manifolds must have crossed each other outside the period two saddle for some parameter $\varepsilon_\gamma \in [17.3, 18.5]$. In fact, it is this change of position of the stable and unstable manifolds that causes the disappearance of the invariant set created in the Hopf bifurcation: initial states starting close to the monetary steady state will follow the stable manifolds and eventually escape to the negative quadrant.

In both cases we have shown that for certain parameters the stable and unstable manifolds have no points of intersection outside the periodic saddles while for other parameters they do have points of intersection outside the saddles. As can been seen from the figures, the dynamics becomes extremely complicated. Let us now formalize cases 1 and 2.

Case 1 (continued) ($\sigma = 0.025$):

Let us first establish a result that guarantees the generic unfolding of transversal homoclinic intersections.

[14] This method finds, up to any prescribed accuracy, orbits on the stable and unstable manifolds as fixed points of a contraction mapping of the space of orbits.

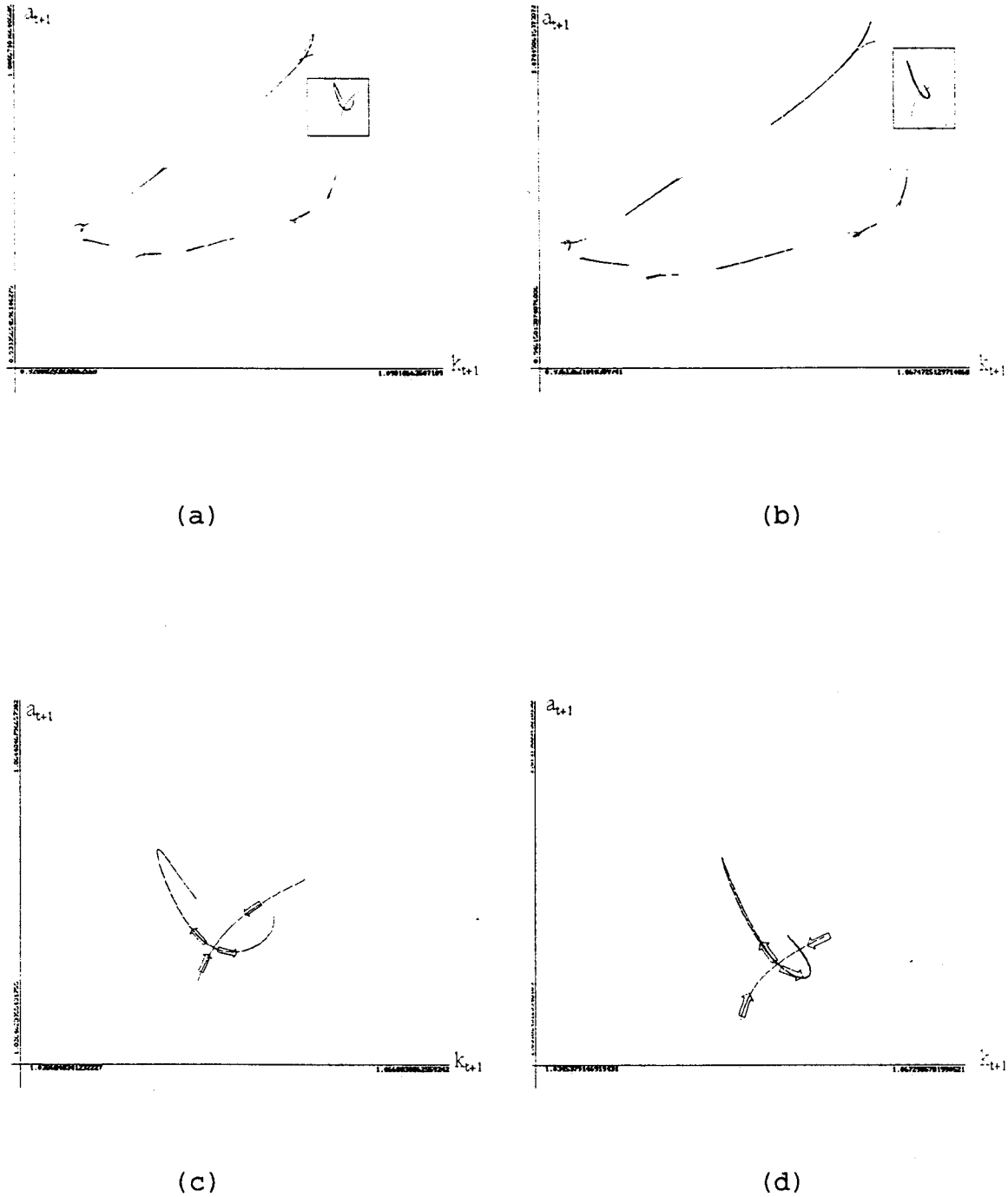

Figure 10: The stable and unstable manifolds of the period 9 saddle orbit. The stable manifolds are marked with arrows directed towards the generating saddle whereas the unstable manifolds are marked with arrows directed away from the generating saddle. (a) For $\varepsilon_\gamma = 8.294$ the stable and unstable manifolds of the period 9 saddle orbit have no points of intersection outside the periodic saddle orbit itself; see also (c) where we have enlarged the boxed region containing one of the saddles. (b) For $\varepsilon_\gamma = 8.314$ the stable and unstable manifolds of the period 9 saddle orbit do have points of intersection outside the periodic saddle orbit itself; in (d) we show an enlargement of the boxed region that contains one of the saddles.

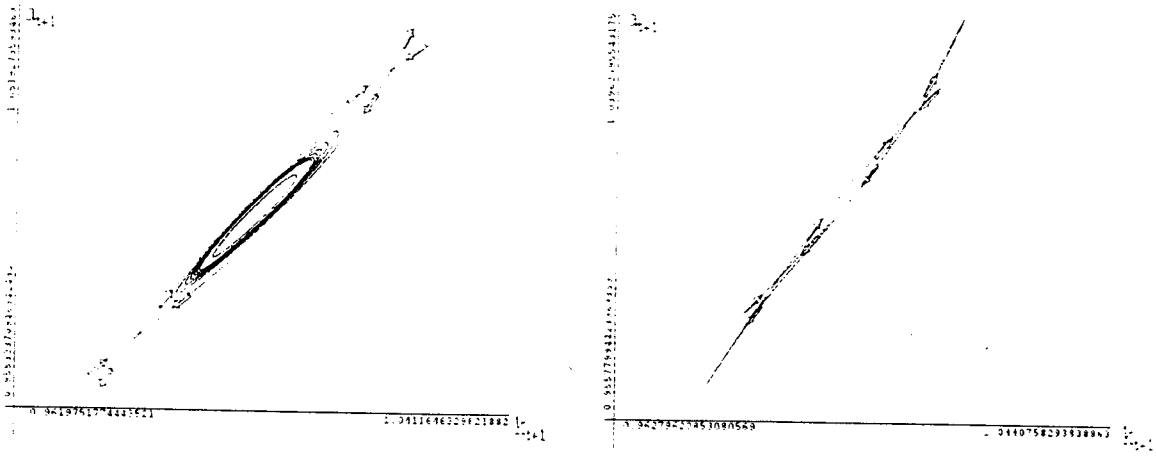

(a) (b)

Figure 11: The stable manifolds are marked with arrows directed towards the generating saddle whereas the unstable manifolds are marked with arrows directed away from the generating saddle; (a) for $\varepsilon_\gamma = 17.2$ the unstable manifolds of the period 2 saddle orbit converge to the attracting invariant set created in the Hopf bifurcation whereas the stable manifolds wander off. In (b) the stable and unstable manifolds have changed position. In fact, the stable manifold now converges to the monetary steady state; all orbits of initial states close to the monetary steady state follow the stable manifolds and eventually escape to the negative quadrant.

Proposition 3.1

The following holds:

- *For $\varepsilon_\gamma = 8.294$ the stable and unstable manifolds of the dissipative period 9 saddle orbit have no points of homoclinic intersection (figures 10a and c).*
- *For $\varepsilon_\gamma = 8.314$ the stable and unstable manifolds of the dissipative period 9 saddle orbit have points of transversal homoclinic intersection (figures 10b and d).*
- *There exist a value $\varepsilon_\gamma \in [8.294, 8.314]$ such that the stable and unstable manifolds of the dissipative period 9 saddle orbit have points of quadratic homoclinic tangency that unfold with non-zero speed.*

Proof: We have checked that for all $\varepsilon_\gamma \in [8.294, 8.314]$ the product of the eigenvalues evaluated at the period 9 saddle is smaller than 0.1. The method that we use to compute the stable and unstable manifolds (cf. DUNRO [11]) guarantees an accurate approximation of true manifolds. Therefore, from figures 10a and c, the stable and unstable manifolds of the period 9 saddle orbit have no non-trivial intersections for $\varepsilon_\gamma = 8.294$ whereas they do have points of non-trivial intersection for $\varepsilon_\gamma = 8.314$ (cf. figures 10b and d). Since our family G_{ε_γ} is two-dimensional, smoothly depending on the parameter, it follows that there exists a value $\varepsilon_\gamma \in [8.294, 8.314]$ for which the stable and unstable manifolds of the period 9 saddle orbit intersect tangentially. Having one point of homoclinic tangency ensures

the existence of infinitely many homoclinic tangencies; at least one of these tangencies is quadratic and unfolds in a non-degenerate fashion (see Palis and Takens [25, Theorem 1 p. 36]). Hence, we have proved the generic unfolding of a non-trivial homoclinic intersection of the stable and unstable manifolds of the period 9 saddle orbit. □

In Palis and Takens [25, Theorem 1 p. 36] it is shown that if there exists a quadratic homoclinic tangency that unfolds generically for say $\hat{\varepsilon}_\gamma$, then one can find an infinite sequence of parameters ε_γ converging to $\hat{\varepsilon}_\gamma$ such that for each parameter in the sequence there exist distinguishable quadratic homoclinic tangencies that also unfold in a non-degenerate manner. So, having one quadratic homoclinic tangency that unfolds generically for $\hat{\varepsilon}_\gamma$ ensures the presence of a whole sequence of ε_γ values for which different quadratic homoclinic tangencies unfold generically. For each such quadratic homoclinic tangency we have, as a consequence of the above discussion, the following result:

Theorem 3.1

For each point of quadratic homoclinic tangency associated with the stable and unstable manifolds of the dissipative period 9 saddle that unfolds generically, there is an $\epsilon > 0$ (small) such that the following holds (where $\hat{\varepsilon}_\gamma$ is the parameter value for which the tangency occurs):

1. *For any $\varepsilon_\gamma \in (\hat{\varepsilon}_\gamma, \hat{\varepsilon}_\gamma \pm \epsilon)$, where we take $\varepsilon_\gamma + \epsilon$ if the tangency unfolds with positive speed, $\varepsilon_\gamma - \epsilon$ if it unfolds with negative speed, there exist transverse homoclinic orbits and therefore infinitely many invariant Cantor sets Λ. Each Cantor set contains infinitely many periodic points, an uncountable set of aperiodic points and dense orbits, all of saddle-type (it is a Smale horseshoe).*

2. *There are countably infinitely many intervals I_i in $(\hat{\varepsilon}_\gamma - \epsilon, \hat{\varepsilon}_\gamma + \epsilon)$ and dense subsets $D_i \subset I_i$ such that for each parameter $\varepsilon_\gamma \in D_i$, G_{ε_γ} has infinitely many coexisting periodic attractors of arbitrary large period (the Newhouse phenomenon). In addition for each arbitrary large $N \geq 1$ there exists an interval $M_N \subseteq (\hat{\varepsilon}_\gamma - \epsilon, \hat{\varepsilon}_\gamma + \epsilon)$ such that for each $\varepsilon_\gamma \in M_N$, G_{ε_γ} has at least N coexisting periodic attractors.*

3. *There is a set of parameters $E \subset (\hat{\varepsilon}_\gamma - \epsilon, \hat{\varepsilon}_\gamma + \epsilon)$ with positive Lebesgue measure such that the map G_{ε_γ} has a strange Hénon-like attractor for each $\varepsilon_\gamma \in E$.*

4. *For $\varepsilon'_\gamma = 8.294$ the stable and unstable manifolds of the period 9 saddle have no non-trivial points of intersection whereas for $\varepsilon''_\gamma = 8.314$ there is a full horseshoe; therefore as ε_γ increases in $(\varepsilon'_\gamma, \varepsilon''_\gamma)$, an infinite number of period doubling and period halving cascades occur.*

Proof: The generic unfolding of homoclinic tangency guarantees the existence of infinitely many transversal homoclinic intersections. From Smale [28] it follows that there exist infinitely many

horseshoes, and assertion 1 follows. Assertions 2 and 3 follow from Newhouse [24] and Mora and Viana [23]. Because of the first and second assertions of proposition 3.1 we can use Yorke and Alligood [34] and Kan, Kocak and Yorke [21] to prove the last assertion of the theorem. □

Case 2 (continued) ($\sigma = 0.05$):

As in the previous case we first establish a result concerning the generic unfolding of transversal homoclinic intersections. In the description of Case 2, we mentioned the intersection between the stable manifold of one saddle and the unstable manifold of the other saddle which compose the period-two cycle (see Fig. 11). The corresponding points of intersection are called *transversal heteroclinic points* or points of *heteroclinic tangency* if the intersection is transversal or tangential, respectively. It can be shown that the occurence of heteroclinic intersections in fact implies that there also exist homoclinic intersections.

Proposition 3.2

The following holds:

- *For $\varepsilon_\gamma = 17.3$ the stable and unstable manifolds of the dissipative period 2 saddle orbit have no points of heteroclinic intersection (figure 11a).*
- *For $\varepsilon_\gamma = 18.5$ the stable and unstable manifolds of the dissipative period 2 saddle orbit have points of transversal heteroclinic intersection (figure 11b).*
- *There exists a value' $\varepsilon_\gamma \in [17.3, 18.5]$ such that the stable and unstable manifolds of the dissipative period 2 saddle orbit both have points of quadratic heteroclinic and homoclinic tangency that unfold with non-zero speed.*

Proof: First we have checked that for $\varepsilon_\gamma \in [17.3, 18.5]$ the product of the eigenvalues of the Jacobian matrix evaluated at the periodic saddle orbit of period 2 is smaller than 0.8. Next, note from figure 11a-b that the stable manifolds do not intersect the unstable manifolds. While increasing the parameter from $\varepsilon_\gamma = 17.3$ to $\varepsilon_\gamma = 18.5$ the stable manifold of one member crosses the unstable manifold of the other member of the period 2 saddle. Using the program DUNRO [11] we have checked that the latter intersection is transversal: there exist points of heteroclinic transversal intersections. Since these heteroclinic intersections are between the stable and unstable manifolds of the same periodic orbit it follows that there also exist points of homoclinic intersection. Due to the fact that horseshoes are structurally stable we know that there must exist an interval of parameters ε_γ for which there exist transversal intersections: there exists an open set of ε_γ values $\psi \subset [17.3, 18.5]$ such that for

each $\varepsilon_\gamma \in \psi$ there exist transversal homoclinic intersections. We have thus proved that for $\varepsilon_\gamma = 17.3$ there are no homoclinic intersections whereas for the interval of parameters ψ there exists transversal homoclinic intersections. Using the same type of arguments as in the proof of proposition 3.1 we know that there also exist a parameter ε_γ for which there are quadratic homoclinic tangencies that unfold with non-zero speed. □

It should be clear from the discussion in this section that the main implications for the dynamics of the model due to these generically unfolding homoclinic intersections are similar to the ones presented in theorem 3.1.

Remark: Throughout this section we have focused on the complexities associated with both the stable and unstable manifolds of the period 9 saddle orbit and a period 2 saddle orbit. In the latter case it is clear that the unfolding of homoclinic tangencies fully accounts for the observed complexities. However, one cannot draw the same conclusion for the period 9 orbit (case 1). In fact, we could replace the period 9 orbit with a periodic saddle orbit with a different period. The (co)existence of different periodic orbits can be understood from the discussion of Arnol'd tongues as well as the work of Aronson, Chory, Hall and McGehee [2]. In fact, to explain the full complexities we have presented in figure 5c-d one also has to take the stable and unstable manifolds of other periodic saddles into account. However, for reasons of brevity and exposition we have omitted this additional analysis.

4 Conclusion

The period-doubling bifurcation theorem and the Hopf bifurcation theorem have frequently been applied to economic models. The former bifurcation in particular has proved to be very useful in showing the existence of complicated global output time paths in one-dimensional general equilibrium models. The Hopf bifurcation theorem however has mostly been utilized in economic modeling to show the existence of (quasi) periodic fluctuations for realistic parameter specifications. Little attention has been paid to its global properties, i.e. for parameters sufficiently far away from the bifurcation point. We have shown in this paper that the invariant circle created in the stable Hopf bifurcation transforms into a strange attractor when an essential parameter of the model is increased "far away" from the bifurcation value. An equivalent way of saying this is that close to the bifurcation value the dynamics of the model is regular whereas it may become very irregular for other parameters. The main methodological contribution of this paper is that we were able to relate this transition from regular to irregular motion to the creation of homoclinic intersections of stable and unstable manifolds of periodic saddle equilibria. Yet another demonstration of the importance of the presence of (periodic) saddle equilibria on the global dynamics of higher-dimensional economic models. Moreover, earlier

numerical findings reported by other authors may be understood within the presented framework. In fact, it seems that a quite general mechanism is at work and we expect that similar phenomena may be encountered in other nonlinear economic models.

References

[1] V.I. Arnol'd (1977): *Loss of stability of self oscillations close to resonances and versal deformations of equivariant vector fields.* Functional Analysis and Applications 11, 1-10.

[2] D.G. Aronson, M.A. Chory, G.R. Hall and R.P. McGehee (1982): *Bifurcations from an invariant circle for two-parameter families of maps of the plane: a computer assisted study.* Communications in Mathematical Physics 83, 303-354.

[3] V. Baladi and M. Viana (1995): *Strong stochastic stability and rate of mixing for unimodal maps*, Informes de matemática, A-115/95.

[4] M. Benedicks and L. Carleson (1991): *The dynamics of the Hénon map.* Annals of Mathematics 33, 73-169.

[5] J. Benhabib and R. Day (1982): *A characterization of erratic dynamics in the overlapping generations model.* Journal of Economic Dynamics and Control 4, 37-55.

[6] J. Benhabib and G. Laroque (1988): *On competitive cycles in productive economies.* Journal of Economic Theory 45, 145-170.

[7] W.A. Brock and C.H. Hommes (1995): *Rational routes to randomness.* Preprint University of Wisconsin, Dpt. of Economics, No. 9506.

[8] G. Cazzavillan, T. Lloyd-Braga and P. Pintus (1995): *Multiple steady states and endogenous fluctuations with increasing returns in production.* To appear in CEPREMAP working papers.

[9] G. Cazzavillan and P. Pintus (1995): *Multiple stationary equilibria and long-run endogenous fluctuations in an overlapping generations economy with increasing returns.* To appear in CEPREMAP working papers.

[10] R.A. Dana and P. Malgrange (1984): *The dynamics of a discrete version of a growth cycle model.* In: Analyzing the structure of econometric models. J.P. Ancot (ed.). Amsterdam: Nijhoff.

[11] DUNRO *(1994): a global bifurcation analyzer.* By D.J. Sands and R.G de Vilder.

[12] R.A. Farmer (1986): *Deficits and cycles.* Journal of Economic Theory 40,77-88.

[13] J. Goeree, C.H. Hommes and H.W. Weddepohl (1995): *Stability and complex dynamics in a discrete tâtonnement model.* Research report AE 10/95, University of Amsterdam, the Netherlands.

[14] J.-M. Grandmont (1985): *On endogenous competitive business cycles.* Econometrica 53, 995-1045.

[15] J.-M. Grandmont (1993): *Expectations driven nonlinear business cycles.* Rheinisch-Westfälische Akademie der Wissenschaften, Vorträge N 397, Westdeutcher Verlag.

[16] J.-M. Grandmont, P. Pintus and R.G. de Vilder (1995): *Capital-labour substitution and competitive endogenous business cycles.* To appear in CEPREMAP working papers.

[17] J. Guckenheimer and P. Holmes (1983): *Nonlinear oscillations, dynamical systems and bifurcations of vector fields.* Springer-Verlag.

[18] A.-J Homburg (1993): *On the computation of hyperbolic sets and their invariant manifolds.* Institut für Angewendte Analyses und Stochastik, preprint no. 68. Berlin.

[19] A.-J. Homburg, D.J. Sands and R.G. de Vilder (1995): *Computing invariant sets.* Submitted for publication (available from the authors).

[20] B. Jullien (1988):*Competitive business cycles in an overlapping generations economy with productive investment.* Journal of Economic Theory 46, 45-65.

[21] I. Kan, H. Koçak and J.A. Yorke (1992): *Antimonotonicty: concurrent creation and annihilation of periodic orbits.* Annals of Mathematics 136, 219-252.

[22] A. Medio and G. Negroni (1994): *Chaotic dynamics in Overlapping generations models with production.* Preprint "Nota Di Lavoro" no. 93.08, Universita Degli Studi Di Venezia, Italy.

[23] L. Mora and M. Viana (1993); *Abundance of strange attractors.* Acta Mathematica 171, 1-71.

[24] S. Newhouse (1974): *Diffeomorphisms with infinitely many sinks.* Topology 13, 9-18.

[25] J. Palis and F. Takens (1993): *Hyperbolocity & sensitive chaotic dynamics at homoclinic bifurcations.* Cambridge University Press.

[26] J. Palis and M. Viana (1994): *High dimension diffeomorphisms displaying infinitely many periodic attractors*, Annals of Mathematics, 140, 207-250.

[27] P. Reichlin (1986): *Equilibrium cycles in an overlapping generations economy with production.* Journal of Economic Theory 40, 89-102.

[28] S. Smale (1963): *Diffeomorphisms with many periodic points.* In Differential and Combinatorial Topology, S. Cairns (ed), pp 63-80. Princeton University Press.

[29] F. Takens (1992): *Abundance of generic homoclinic tangencies in real-analytic diffeomorphisms.* Bullitin Soc. Bras. Mat.

[30] R.G. de Vilder (1995): *Complicated endogenous business cycles under gross substitutability.* To appear in the Journal of Economic Theory. (Available as No. 9501 CNRS/CEPREMAP (Paris, France) working papers).

[31] R.G. de Vilder (1995): *Endogenous business cycles.* Ph.D thesis Tinbergen Institute Research series n. 96, The Netherlands.

[32] S. Wiggins (1990): *Introduction to applied nonlinear dynamical systems and chaos.* Springer-Verlag.

[33] M. Woodford (1986): *Stationary sunspot equilibria in a finance constrained economy.* Journal of Economic Theory 40, 128-137.

[34] J.A. Yorke and K.T. Alligood (1983): *Cascades of period-doubling bifurcations: a prerequisite for horseshoes.* Bulletin of the American Mathematical Society 9, 319-322.